Passive larval transport explains recent gene flow in a Mediterranean gorgonian

Mariana Padrón, Federica Costantini, Sandra Baksay, Lorenzo Bramanti, Katell Guizien

Larval transport explains contemporary gene flow in a Mediterranean gorgonian

Mariana Padrón[1], Federica Costantini[2], Sandra Baksay[3], Lorenzo Bramanti[1], Katell Guizien[1*]

[1] Sorbonne Universités, UPMC Univ Paris 06, CNRS, Laboratoire d'Ecogéochimie des Environnements Benthiques (LECOB), Observatoire Océanologique, 66650, Banyuls sur Mer, France.

[2] Dipartimento di Scienze Biologiche, Geologiche ed Ambientali (BiGeA) & Centro Interdipartimentale di Ricerca per le Scienze Ambientali (CIRSA), Università di Bologna, ULR CoNISMa, Via S. Alberto 163, I-48123 Ravenna, Italy.

[3] Laboratoire Evolution et Diversité Biologique EDB, CNRS, Université Toulouse III Paul Sabatier, F-31062 Toulouse, France.

*Corresponding author: tel: +33 468887319; e-mail: guizien@obs-banyuls.fr;

ORCID: 0000-0001-9884-7506

Keywords: marine connectivity, Pelagic Larval Duration, genetic structure, Marine Protected Areas, hydrodynamic model, Gulf of Lion.

Abstract

Understanding the patterns of connectivity is required by the Strategic Plan for Biodiversity 2011-2020 and will be used to guide the extension of marine protection measures. Despite the increasing accuracy of ocean circulation modeling, the capacity to forecast the population connectivity of sessile benthic species with dispersal larval stages can be limited due to the potential effect of demographic filters acting before or after dispersal, which modulate offspring release or settlement, respectively. We applied an interdisciplinary approach that combined demographic surveys, genetic methods (assignment tests and coalescent-based analyses) and larval transport simulations to test the relative importance of demographics and ocean currents in shaping the contemporary patterns of gene flow among populations of a Mediterranean gorgonian (*Eunicella singularis*) in a fragmented rocky habitat (Gulf of Lion, NW Mediterranean Sea). We show that larval transport is a dominant driver of gene flow among the populations, and significant correlations were found between the contemporary gene flow and recent larval transport when the pelagic larval durations (PLDs) ranged from 7 to 14 days. Our results suggest that PLDs that efficiently connect populations distributed over a fragmented habitat are filtered by the habitat layout within the species competency period. Moreover, a PLD ranging from 7 to 14 days is sufficient to connect the fragmented rocky substrate of the Gulf of Lion. The rocky areas located in the center of the Gulf of Lion, which are currently not protected, were identified as essential hubs for the distribution of migrants in the region. We encourage the use of a range of PLDs instead of a single value when estimating larval transport with biophysical models to identify potential connectivity patterns among a network of marine protected areas or even solely a seascape.

Introduction

The Strategic Plan for Biodiversity 2011-2020 aims to conserve 10% of the ocean through well-connected systems of marine protected areas (MPAs) by 2020 (Aichi Target 11,

https://www.cbd.int/sp/targets/rationale/target-11/). Hence, understanding the degree and patterns of connectivity among existing MPAs and areas where protection could be extended becomes urgent. Connectivity is also known as the mechanism through which populations of sessile marine species, and particularly coral species, can recover after local and global disturbances (Roberts 1997; Hanski 1998; Cowen et al. 2000). In the context of global change, relating contemporary connectivity to the seascape processes that shape the spatial distribution of marine species is essential for the design of effective biodiversity conservation strategies.

Seascape processes that drive population connectivity of sessile species with a larval dispersal stage, such as corals or gorgonians, should include both seabed geomorphology and dynamic hydrography (Manderson 2016). Correlations at the local scale between demographic population descriptors and the environment may, indeed, not be sufficient, and the successful exchange of individuals between distant locations (i.e., connectivity) should be included. Recent studies on seascape connectivity have focused on evaluating how larval transport drives genetic patterns across the seascape using a combination of biophysical and genetic approaches (see Liggins et al. 2013 for a review). Nonetheless, Selkoe et al. (2016) reported that only 31% of the analyzed studies found ocean currents to be a good predictor of gene flow patterns and ascribed this poor predictability to inappropriate scales in genetic sampling. These findings suggest that demographic and genetic connectivity of benthic sessile species, for which connectivity among populations only occurs during the larval dispersive stage, are affected by several processes acting as successive biological filters at different temporal and spatial scales along their life cycles from spawning to reproduction by the settled individuals (Pineda 2007).

Prior to dispersal, population size and fecundity are among the key factors that determine the number of emigrant offspring and have been shown to influence connectivity patterns in marine species (Treml et al. 2012; Dawson et al. 2014). After dispersal, gene flow among areas that are well connected through larval transport can be limited by settlement regulation due to space limitations (Roughgarden et al. 1985). However, the primary filter of connectivity is larval

transport, which is notably driven by the amount of time that larvae spend being transported by ocean currents, otherwise known as the pelagic larval duration (PLD). Hence, the PLD has been the primary factor considered in biophysical modeling when attempting to differentiate dispersal distance capabilities among different species (Shanks et al. 2003).

Genetic studies have tested the relationship between realized connectivity (gene flow) and the PLD following the same reasoning, and the results have led to contrasting conclusions (Kinlan and Gaines 2003; Weersing and Toonen 2009; Riginos et al. 2011, D'Aloia et al. 2015). Several arguments have been invoked to explain the absence of a relationship between PLD and realized dispersal distance and migration rates, with some arguments referring to the way in which realized connectivity is inferred from measures of genetic differentiation among populations. For instance, the inverse relationship between the most common metric of genetic differentiation, F_{ST}, and the migration rate (Wright's Island Model 1931), may be blurred by the uncertainty of the estimation of the effective size of the population (Faurby and Barber 2012). However, the failure to identify a relationship between PLD and realized connectivity is more likely explained by the lack of unequivocal correlation between PLD and dispersal distance. In fact, the variability of ocean currents (Cowen et al. 2006, Guizien et al. 2014), larval behavior (Guizien et al. 2006, Paris et al. 2007) and larval mortality (Cowen et al. 2000) can lead to very different dispersal patterns given the same PLD. Moreover, for any given species, PLD does not have a single value, but it varies along a competency window (Arnold and Steneck 2011), within which successful recruitment can occur at any time once a suitable habitat is found along the dispersal pathway.

To determine which biological filters transform larval release into gene flow (potential into realized connectivity), we used one of the most abundant and conspicuous species of the rocky sublittoral zone in the northwestern Mediterranean Sea, the white gorgonian *Eunicella singularis*.

In the hydrodynamic province of the Gulf of Lion (NW Mediterranean, Rossi et al. 2014),

105 the spatial distribution of *E. singularis* is discontinuous (Gori et al. 2011) due to fragmentation of
106 the rocky habitat (Aloisi et al. 1973). *E. singularis* is believed to play an important ecological role
107 due to its erect structure, which provides habitat for the local epifauna and increases the biomass
108 and diversity of the rocky community (Ballesteros 2006; Mitchell et al. 1992). Furthermore, its
109 indirect economic value due to its contributions to shaping the seascape and attracting SCUBA
110 diving and fishing activities makes *E. singularis* a species of interest in the monitoring plans of
111 all MPAs in the Gulf of Lion. *E. singularis* is a long-lived (up to 15 years) internal brooding ses-
112 sile species. Lecitotrophic larvae (planulae) are released once a year in June-July (Théodor 1967;
113 Weinberg and Weinberg 1979). Larvae can survive up to 122 days in *ex situ* experiments in the
114 absence of predation (Théodor 1967), with 50% to 80% survival after 40 days (K. Guizien, *Per-*
115 *sonal communication*). Competency for recruitment was observed after a few days and lasted up
116 to a few weeks (L. Bramanti, *Personal communication*). Such larval traits suggest a wide disper-
117 sive potential of the species.

118 In the present study, we propose a methodological approach that combines demographic,
119 biophysical and genetic methods to test the relationship between the dispersive potential of a ses-
120 sile benthic species and the effective gene flow in a fragmented habitat layout. The study aims to
121 (1) assess the genetic structure of *Eunicella singularis* within the fragmented habitat of the Gulf
122 of Lion, (2) test the role of demographic filters (i.e., reproductive output and intra-specific recruit-
123 ment limitations) in shaping gene flow, and (3) test the significance of various PLD-driven larval
124 transport modes in shaping the spatial pattern of gene flow.
125
126 **MATERIAL AND METHODS**
127 **Study area and regional hydrodynamics**
128 The Gulf of Lion (hereafter GoL) is a large (~100 km), microtidal continental shelf with a
129 100-km radius located in the northwestern Mediterranean Sea (Figure 1). The first 30 meters of
130 the bathymetry is mainly covered by soft sandy sediment; however, fragmented patches of hard

substrate can be found in the eastern (Côte Bleue), central (Plateau des Aresquiers and Cap d'Agde), and western (Cap Leucate and Côte Vermeille) parts of the gulf (Aloisi et al. 1973). Circulation in the GoL is driven by three main forces: 1) strong continental winds from the north (Mistral) and the northwest (Tramontane) that frequently generate upwelling and downwelling along the coast, as well as transient currents and eddies; 2) the Northern Current (NC), which usually flows westward along the shelf break of the GoL from the Ligurian Sea to the Catalan Sea; 3) river inputs, particularly from the Rhône, that deliver freshwater and high nutrient and organic matter loads (Millot 1990; Hu et al. 2009; Campbell et al. 2013).

Numerical simulations at the basin scale have identified that the GoL is an isolated hydrodynamic province, with the Northern Current acting as a hydrodynamic barrier that limits the transport of particles across the shelf break (Rossi et al. 2014). Large-scale flow limits entries into the Gulf of Lion up to a 60-day PLD from the east and up to a 30-day PLD from the west. Moreover, despite an overall westward drift leading to large sediment exports through western canyons (Ulses et al. 2008), persistent anticyclonic eddies are observed in the southwestern part of the GoL during the summer (Hu et al. 2009), and connectivity patterns within the Gulf of Lion stabilize after 3 weeks.

Sampling design

From July 2013 to October 2014, detectable colonies (taller than 1 cm) of *Eunicella singularis* were counted and sampled at 17 geo-referenced stations distributed along the GoL, from the Côte Bleue to the Côte Vermeille (Table 1) (Figure 1). The stations were distributed along four rocky habitat patches separated by large areas of sandy bottom (Côte Bleue, Plateau des Aresquiers, Cap d'Agde and Côte Vermeille) at depths between 15 and 35 meters. The distance between stations varied from less than 1 km to 180 km. The population size structures were similar in the four rocky habitat patches, with 25% of the colonies smaller than 5 cm, 55% of the colonies between 5 and 20 cm and 20% of the colonies taller than 20 cm (L. Bramanti, *Personal communication*). The number of stations sampled in each habitat patch varied according

157 to the along-shore extension of *E. singularis* coverage of the rocky bottom (L. Bramanti,
158 *Personal communication*). In Côte Bleue, where the smallest coverage of *E. singularis* was
159 found, only three stations were sampled; in Plateau des Aresquiers and Cap d'Agde, four stations
160 were sampled, while six stations were sampled in the Côte Vermeille.

161 The mean population density at each station was calculated from colony counts in 4
162 quadrats (1 m^2 each). For each station, the 4 quadrats were located 5 m from the geo-referenced
163 station, one in each of the four cardinal directions. Small apical fragments (<3 cm) of all colonies
164 of *E. singularis* that were counted at each station were collected, preserved in 95% ethanol and
165 kept at 6 **°C** until DNA extraction. For the present study, 13 to 36 colonies per station were
166 randomly selected and genotyped, for a total of 434 colonies.

167 **Genetic diversity and population structure**

168 All colonies were genotyped at eight microsatellite loci specifically developed for *E.*
169 *singularis*: C21, C30 and C40 (Molecular Ecology Resources Primer Development Consortium
170 2010) and *E. verrucosa*: Ever003, Ever004, Ever009, Ever013 and Ever014 (Holland et al. 2013)
171 after DNA extraction (Appendix S1). The scoring of the alleles was carried out using
172 GeneMapper v.3.7 software (Applied Biosystems). We calculated the summary statistics of the
173 genetic diversity (allelic richness, observed heterozygosity, expected heterozygosity), and tested
174 for departure from the Hardy-Weinberg equilibrium, linkage disequilibrium and the presence of
175 null alleles (Appendix S1). The statistical power to detect the level of genetic variation among
176 populations was estimated using Powsim v.4.1 (Ryman and Palm 2006). The spatial genetic
177 structure of *E. singularis* was analyzed by testing for the presence of a pattern using the isolation
178 by distance (IBD) and the Loiselle kinship coefficient (Appendix S1). The patterns of population
179 genetic structure were analyzed using F_{ST}, a Bayesian clustering method that identifies clusters of
180 individuals who share similar patterns of variation (Structure v.2.3.4; Pritchard et al. 2000) and a
181 hierarchical analysis of molecular variance (AMOVA). For details, see the Methods in Appendix
182 S1.

183 **Contemporary gene flow**

184 The genotyped individuals from the 17 stations were clustered into 4 groups defined by
185 habitat discontinuity, corresponding to the four largest rocky habitat patches (Côte Vermeille,
186 Cap d'Agde, Plateau des Aresquiers and Côte Bleue). Contemporary gene flow over the last 2-3
187 generations was estimated in the form of matrices containing migration rates including a proxy of
188 self-recruitment among these 4 clusters using BayesAss 3.0 applied on multilocus genotypes
189 (Wilson and Rannala 2013). It is important to note that the BayesAss 3.0 output is the proportion
190 of individuals in the destination population that is descendant from a source population.
191 The confidence intervals and the uncertainty values around the average migration rates were
192 estimated (Appendix S1).

193 **Recent larval transport**

194 Using the 3D ocean model Symphonie (S-2010 release 26, at http://sirocco2.omp.obs-
195 mip.fr/outils/Symphonie/Accueil/SymphoAccueil.htm), high-resolution flow simulations were
196 carried out and used for larval dispersal simulations (Appendix S1). The latter were upscaled to
197 the larval transport matrices for single reproductive events. Larval transport matrices contain
198 transfer rate values defined as the proportion of larvae (neutrally buoyant particles) released from
199 a source habitat patch (row) during a given release period that reach a destination habitat patch
200 (column) after a given PLD. Fifteen variations of larval transport matrices were established per
201 PLD, with each variant corresponding to a non-overlapping weeklong release period in June (five
202 variants per year) over three years (2010, 2011, 2012, Appendix S1). Six weeks of dispersal were
203 simulated and eight PLD values ranging from 3.5 to 42 days were tested. The PLD range that was
204 tested was greater than the period during which *Eunicella singularis* larvae competency for
205 recruitment as observed in laboratory experiments (L. Bramanti, *Personal Communication*).
206 Moreover, the maximum PLD tested in the present study (42 days) was longer than the time
207 required to observe stable connectivity patterns within the Gulf of Lion (Briton et al., submitted).

208 **Comparison between larval transport and gene flow**

With gene flow being estimated as the proportion of individuals in the destination population that is a descendant from a source population, and larval transport being the proportion of the larvae released from a source population that arrives in a destination population, comparing gene flow and larval transport requires a series of data transformations (see details in Appendix S1). Briefly, as the actual number of larvae released from a source population is unknown, the transformation of larval transport into the number of larvae reaching a destination population is not possible. Hence, gene flow was transformed into the proportion of migrants that leaves a source population and arrives at each destination population. For each PLD, recent larval transport was estimated as the average of the 15 larval transport matrix variants (one for each single reproductive event). Recent larval transport matrices were normalized so that the sum of the destination probabilities from the same source (i.e., all columns within each row) was equal to one, which removed the proportion of larvae dispersed out of the 4 habitat patches sampled for genetics as this proportion is not included in the gene flow assessment. It is worth noting that after these normalizations, for both the gene flow and larval transport matrices, only rows, not columns, are statistically independent. Hence, the significance of the Pearson product-moment correlations (excluding diagonal terms, i.e., retention rates) between the contemporary gene flow and recent larval transport matrices (4x4) was tested using a Mantel test (Mantel 1967) for all 24 possible permutations, after modifying the random QAP.m Matlab routine by Puck Rombach (2011). In addition, the determination coefficient between contemporary gene flow and recent larval transport was computed including diagonal terms, i.e., retention rates.

Relationship between population density and migration

Finally, the effect of demographic filters on the number of migrants (see calculation in Appendix S1) was tested, namely, the modulation of emigrants by reproductive output from the source populations and the modulation of immigrants by settlement limitation in the destination populations. Two correlation analyses were performed to test the relationship between 1) the number of contemporary emigrants from a source habitat patch (sum of migrants number by row)

and the mean population density in that source (proxy of reproductive output given the same population size structure in all habitat patches), and 2) the number of contemporary immigrants to a destination habitat patch (sum of migrant numbers by column) and the mean population density in that destination patch (proxy of intra-specific competition). All statistical analyses were conducted in Matlab (R2012a).

RESULTS

Genetic diversity and population structure

All sampled individuals were included in the analysis (no identical multilocus genotypes). All loci were polymorphic, with more than 4 alleles among stations on average and from 5 to 13 alleles over all loci, which is comparable to the degree of polymorphism obtained by Holland et al. (2013). Linkage disequilibrium was not observed (Appendix S2, Table A2). The observed and expected heterozygosities were similar among stations with no significant heterozygote excesses, but there were significant heterozygote deficits across two populations (CV1 and CA1) (Appendix S2, Table A2) and in two of the eight loci (Ever003 and C40) (Appendix S2, Table A3). The frequency of null alleles was negligible (Appendix S2, Table A3).

The overall F_{ST} value was low (0.04), and almost all pairwise F_{ST} values among stations were significantly different (P-value < 0.001) (Appendix S2, Table A4). Nei's genetic distance values were closer among the stations within habitat patches than between them (Figure 2). While the stations in Côte Bleue and Cap d'Agde-Plateau des Aresquiers are close to each other, the stations in the Côte Vermeille (CV) appear more scattered along the first axis, with one station (CV5) falling near the stations of Cap d'Agde and Plateau des Aresquiers (CA and PA, respectively).

The Bayesian clustering analysis identified three genetic clusters (K = 3) (mean LnP(K) = -7532.99; Delta K = 25.09). The resulting clustering partially corresponded to the rocky habitat fragmentation in the region (Figure 3): Côte Vermeille (6 stations), Cap d'Agde and Plateau des

261 Aresquiers (8 stations), and Côte Bleue (3 stations). Some individuals in Côte Vermeille depicted
262 higher similarity to individuals from Cap d'Agde and Plateau des Aresquiers rather than to other
263 individuals in Côte Vermeille. The results of the AMOVA confirmed the clustering structure ($P <$
264 0.001) (Appendix S2, Table A5).

265 The correlation between $F_{ST} / (1-F_{ST})$ and the logarithm of the geographic distance ($R^2 =$
266 0.28; P-value = 0.01) was significant but low among the 17 stations in the GoL and was not
267 significant among the 4 patches defined according to rocky habitat fragmentation ($R^2 = 0.81$; P-
268 value = 0.100) (Appendix S2, Figure A2). The estimated maximum size of the genetic patch
269 based on Loiselle's kinship coefficient was 30 km, which is larger than the maximum size of any
270 of the habitat patches in the Gulf of Lion (Appendix S2, Figure A3).

271 **Contemporary gene flow**

272 Figure 4 shows the spatial patterns of the number of contemporary migrants among the 4
273 separated habitat patches in the GoL. The uncertainty of the migration pattern, following an error
274 metric adapted from the Euclidean matrix norm (see details in Appendix S1), was below 25%.
275 Local retention dominated over emigration in all habitat patches. However, local retention was
276 much lower in Côte Bleue (mean = 51 migrants, CI (95%) = 48 – 52 migrants) compared to all
277 other habitat patches (from 90 to 121 migrants) and was comparable to the value of emigration
278 from Cap d'Agde (45 ± 14 migrants). Cap d'Agde acted as a hub, distributing migrants to both
279 Côte Vermeille (westward) (mean = 16 migrants, CI (95%) = 6-19 migrants) and Plateau des
280 Aresquiers (eastward) (mean = 28 migrants, CI (95%) = 17-34 migrants).

281 **Relationship between population density and migration**

282 Neither the number of contemporary emigrants coming from a habitat patch (Figure 5A)
283 nor the number of contemporary immigrants arriving to a habitat patch (Figure 5B) showed a
284 significant correlation with the population density of the source ($R^2 = 0.203$, $P > 0.05$) or the
285 destination ($R^2 = 0.787$, $P > 0.05$) habitat patch, respectively.

Although the lowest number of emigrants corresponded to the source habitat patch with the lowest population density, the opposite was not true. The highest number of emigrants did not come from the habitat patch with the highest population density. The number of immigrants did not decay with increasing population density in the destination habitat patch but conversely increased. However, a similar number of immigrants were found in the destination habitat patches with quite different population densities.

Comparison between recent larval transport and contemporary gene flow

In the following section, both larval transport and gene flow have been normalized for each source population and are subsequently no longer comparable between different source populations. Recent larval transport varied greatly among the PLDs ranging from 3.5 to 42 days: from a scenario of high local retention within all habitat patches to a scenario of high levels of larval transport among most habitat patches, except Côte Vermeille (Figure 6A to 6E). Larval transport was restricted to the exchange between Cap d'Agde and Plateau des Aresquiers for the shortest PLD tested (3.5 days, Figure 6A), and increased in a westward direction for the PLDs longer than 14 days (Figures 6D, 6E and data not shown). For the PLDs of 7 and 10.5 days (Figure 6B and 6C), larval transport was westward from Plateau des Aresquiers and Côte Bleue, but both westward and eastward from Cap d'Agde. Moreover, it is interesting to note that the local retention decayed more rapidly in Cap d'Agde compared to the other habitat patches due to efficient larval export towards the closest habitat patches of Plateau des Aresquiers and Côte Vermeille. This pattern matched the one observed for contemporary gene flow particularly well (Figure 6F).

The Mantel test showed a significant correlation (Mantel statistics <5%) between contemporary gene flow and recent larval transport (excluding retention rates) only for the PLDs ranging from 7 to 14 days with a determination coefficient (including retention rates) larger than 50% (Figure 7). However, the determination coefficient between contemporary gene flow and recent larval transport, which includes retention rates, was also high for a PLD of 3.5 days (R^2

>0.95). Interestingly, the determination coefficient did not decrease monotonically with PLD but rather peaked at a PLD of 7 days ($R^2 = 0.98$).

DISCUSSION

Habitat fragmentation fails to explain regional genetic structure of Eunicella singularis *in the Gulf of Lion*

The analysis of the genetic differentiation of groups of *Eunicella singularis* colonies among a wide range of spatial scales (from less than 1 km to 180 km) showed high levels of genetic variability at small scales with a deficit of heterozygotes at some stations, as reported previously for the same species (Costantini et al. 2016) and in other Mediterranean gorgonians such as *Paramuricea clavata* (Mokhtar-Jamaï et al. 2011) and *Corallium rubrum* (Costantini et al. 2007). In these studies, genetic patchiness was attributed to inbreeding, putatively due to the low dispersal ability of the larvae. However, the genetic clustering analysis of *E. singularis* populations in the GoL revealed strong similarity among the individuals sampled in Cap d'Agde and Plateau des Aresquiers, which are separated by 30 km of sandy bottom that is unsuitable for colonization by the species (Weinberg 1978). Moreover, one station in the Côte Vermeille cluster displayed higher similarity to the stations at Cap d'Agde and Plateau des Aresquiers than to the other stations in Côte Vermeille. These similarities to the genetic profiles of distant stations led to an estimated genetic patch size of 30 km, meaning that the individuals found within an area of 30 km would be more genetically related than those taken randomly from any further distance. These results, together with the absence of genetic structure among *E. singularis* populations found within 15 km (Costantini et al. 2016) in the neighboring hydrodynamic province (Balearic Sea, Rossi et al. 2014), suggest that the heterozygote deficit in the *E. singularis* populations in the GoL should be attributed to on-going migration among open populations rather than to inbreeding in closed populations. Nevertheless, migration was not explained by isolation by distance (Sexton et al. 2013; Nanninga et al. 2014; Thomas et al. 2015), which pinpoints the limitation of using the

IBD model to explain the chaotic genetic patchiness resulting from larval dispersal via ocean flow (Selkoe et al. 2010). Indeed, undirected pairwise F_{ST} is not a good measure of genetic distance when migration among populations is asymmetrical (Beerli 1998; Broquet and Petit 2004; van Strien et al. 2015). In such a case, assignment tests or coalescent methods should be used to describe gene flow patterns and determine the factors shaping them (Manel et al. 2005).

Gene flow is determined by larval transport

We tested three major successive filters that potentially influence gene flow during larval dispersal among habitat patches. First, the number of emigrants of *E. singularis* within separated habitat patches in the GoL was not explained by reproductive output. Second, the number of immigrants was not limited by settlement regulation due to intra-specific competition, although this mechanism is often presented (Roughgarden et al., 1985; Padron and Guizien 2015). It is interesting to note that conversely, the population density in the destination habitat patch increased with the number of immigrants, suggesting that the population densities observed in the GoL were below habitat saturating capacity. Third, larval transport explained a large portion of the gene flow among populations. In the GoL, the determination coefficient between contemporary gene flow and recent larval flow was extremely high for a 7-day larval transport duration among four habitat patches.

The combination of the absence of a density-dependent regulation of *E. singularis* migrants in the GoL and the fact that gene flow is driven by unsteady larval transport support the alternate dominance of recruits vs. adult colony populations hypothesis that was observed for the same species along the Costa Brava (NW Mediterranean, Spain) (Linares et al. 2008). The strong correlation between recent larval transport and contemporary gene flow found in this study contrast with other studies based on the correlation with multi-generational gene flow (White et al. 2010; Alberto et al. 2011). This underpins the importance of testing the relationship between larval transport and gene flow estimated for a single dispersive event rather than for multiple

363 generations. Moreover, estimations at the single dispersive event scale enabled the discrimination
364 of the efficiency of different PLDs in connecting populations.

365 *The environment filters the PLDs that connect populations*

366 E*x situ* observations of survival expectancy and competency duration of *E. singularis*
367 larvae (up to 40 days, K. Guizien and L. Bramanti, *Personal Communication*) suggest that all
368 tested PLDs were equally probable in the absence of predation. In such a case, one would expect
369 gene flow to be a composite of larval transport for all PLDs. However, gene flow among
370 populations was best explained by PLDs ranging from 7 to 14 days in the habitat configuration of
371 the GoL, and led to a spatially structured genetic population despite high local chaotic genetic
372 patchiness. Similar finding was obtained among lobster populations along the Californian coast
373 and related to upwelling intensity (Iacchei et al. 2013). In the present case of a lecithotrophic
374 larva with a wide competence window, we suggest that larval mortality significantly altered larval
375 transport patterns for periods longer than 14 days (Cowen et al. 2000). Correlatively, it suggests
376 that mortality, particularly by predation, on *Eunicella singularis* larvae (2-3 mm) can be
377 neglected up to a 14-day PLD in the GoL.

378 Treml et al. (2012) found that longer maximum PLDs lead to a more connected seascape
379 on an ocean basin scale. The study claimed that maximum PLD is a good predictor of larval
380 transport at large geographic scales (200-500 km) but a poor predictor at a mesoscale (<200 km).
381 Our study evaluated the larval transport patterns among populations at a regional scale (up to 180
382 km) and showed that the PLD-indexed larval transport could significantly determine gene flow at
383 a mesoscale. Our findings suggest that several PLDs should be tested along the competency
384 period of a species rather than the average or the maximum PLD to provide a more accurate
385 assessment of the importance of larval transport in shaping gene flow among sessile benthic
386 species (D'Aloia et al. 2015).

387 *Implications for conservation*

388 Our results have important implications for regional conservation and the spatial

management of benthic sessile species in the GoL. Empirical gene flow patterns allow for the identification of key habitat patches of *E. singularis*: the high levels of gene flow between Cap d'Agde and Plateau des Aresquiers, along with transfers to other habitat patches, suggest that these two areas play a pivotal role in the spread of *E. singularis* in the region. Furthermore, the significant correlation between contemporary gene flow and recent larval transport for a PLD ranging from 7 to 14 days suggests that Cap d'Agde and Plateau des Aresquiers could be important sites for any species with similar dispersive traits (PLD, larval behavior, or reproductive period) dwelling on the same rocky substrate, as they should follow the same potential connectivity patterns. Hence, we advocate for enforcing the protection of those sites already identified as important for the regional persistence of soft-bottom species (Guizien et al. 2014), which also appears to be functionally important for the life cycle of some rocky species.

In summary, the methodological approach presented in this study highlights the hidden determinism within the apparent genetic chaos by incorporating interdisciplinary data (demography and ocean currents) and applying accurate genetic tools (coalescent-based analyses) to evaluate the gene flow among populations.

Authors' Contributions

M.P., L.B., and K.G. designed the study. S.B. performed all the laboratory work. M.P., F.C. and K.G. analyzed all the data. All authors contributed to the writing of the manuscript.

Data Accessibility

Microsatellite genotypes will be made available in Dryad.

Acknowledgements

This work was (co-) funded through a MARES Grant. MARES is a Joint Doctorate program selected under Erasmus Mundus coordinated by Ghent University (FPA 2011-0016). Check www.-

mares-eu.org for additional information. This work was also partially funded by the French National Program LITEAU IV of the Ministère de l'Ecologie et de l'Environnement Durable under project RocConnect—Connectivité des habitats rocheux fragmentés du Golfe du Lion (PI, K. Guizien, Project Number 12-MUTS-LITEAU-1-CDS-013. The authors particularly thank the scientific managers of the Gulf of Lion MPA: S. Blouet, E. Charbonnel, B. Ferrari and J. Payrot for valuable interactions during the study design. The authors gratefully acknowledge the helpful assistance during sampling of R. Bricout, F. Cornette, S. Fanfard, B. Hesse, C. Labrune, L. Lescure, J.-C. Roca, P. Romans, and the staff of the Réserve Naturelle Marine de Cerbère-Banyuls, Aire Marine Protégée Agatoise, Parc Naturel Marin du Golfe du Lion and Parc Marin de la Côte Bleue. We also acknowledge American Journal Experts for English editing service.

425

426 **REFERENCES**

427 Alberto F, Raimondi P, Reed D, Watson J, Siegel D, Mitarai S, Coelho N, Serrão E (2011) Isola-
428 tion by oceanographic distance explains genetic structure for *Macrocystis pyrifera* in the
429 Santa Barbara Channel. Molecular Ecology 20:2543–2554.

430 Aloisi J, Got H, Monaco A (1973) Carte géologique du précontinent languedocien au
431 1/250000ième. Enschede: International Institute for Aerial Survey and Earth Sciences,
432 Netherlands.

433 Arnold SN, Steneck R (2011) Setting into an increasingly hostile world: the rapidly closing "re-
434 cruitment window" for corals. PLoS ONE 6:e28681.

435 Ballesteros E (2006) Mediterranean coralligenous assemblages: a synthesis of present knowledge.
436 Oceanography and Marine Biology 44:1–74.

437 Beerli P (1998) Estimation of migration rates and population sizes in geographically structured
438 populations. In: Carvalho G. (eds) Advances in Molecular Ecology (NATO Science Series
439 A: Life Sciences, Vol. 306). IOS Press, Amsterdam, pp 39–53.

440 Beerli P, Felsenstein J (2001) Maximum likelihood estimation of a migration matrix and effec-
441 tive population sizes in *n* subpopulations by using a coalescent approach. Proceedings of the
442 National Academy of Sciences 98:4563–4568.

443 Broquet T, Petit E (2004) Quantifying genotyping errors in noninvasive population genetics.
444 Molecular Ecology 13:3601–3608.

445 Campbell R, Diaz F, Hu Z, Doglioli A, Petrenko A, Dekeyser I (2013) Nutrients and plankton
446 spatial distributions induced by coastal eddy in the Gulf of Lion. Insights from a numerical

447 model. Progress in Oceanography 109:47–69.

448 Costantini F, Fauvelot C, Abbiati M (2007) Genetic structuring of the temperate gorgonian coral
449 (*Corallium rubrum*) across the western Mediterranean Sea revealed by microsatellites and
450 nuclear sequences. Molecular Ecology 16:5168–5182.

451 Costantini F, Gori A, López-González P, Bramanti L, Rossi S, Gili J-M, Abbiati M (2016) Lim-
452 ited genetic connectivity between gorgonian morphotypes along a depth gradient. PLoS ONE
453 11:e0160678.

454 Cowen R (2000) Connectivity of marine populations: open or closed? Science 287:857–859.

455 Cowen R (2006) Scaling of connectivity in marine populations. Science 311:522–527.

456 D'Aloia C, Bogdanowicz S, Francis R, Majoris J, Harrison R, Buston P (2015) Patterns, causes,
457 and consequences of marine larval dispersal. Proceedings of the National Academy of Sci-
458 ences 112:13940–13945.

459 Dawson M, Hays C, Grosberg R, Raimondi P (2014) Dispersal potential and population genetic
460 structure in the marine intertidal of the eastern North Pacific. Ecological Monographs
461 84:435–456.

462 Faurby S, Barber P (2012) Theoretical limits to the correlation between pelagic larval duration
463 and population genetic structure. Molecular Ecology 21:3419–3432.

464 Gori A, Rossi S, Berganzo E, Pretus J, Dale M, Gili JM (2011) Spatial distribution patterns of the
465 gorgonians *Eunicella singularis*, *Paramuricea clavata*, and *Leptogorgia sarmentosa* (Cape
466 of Creus, Northwestern Mediterranean Sea). Marine Biology 158:143–158.

467 Guizien K, Brochier T, Duchêne JC, Koh BS, Marsaleix P (2006) Dispersal of *Owenia fusiformis*

larvae by wind-driven currents: turbulence, swimming behaviour and mortality in a three-dimensional stochastic model. Marine Ecology Progress Series 311:47–66.

Guizien K, Belharet M, Moritz C, Guarini JM (2014) Vulnerability of marine benthic metapopulations: implications of spatially structured connectivity for conservation practice in the Gulf of Lions (NW Mediterranean Sea). Diversity and Distributions 1–11.

Hanski I (1998) Metapopulation dynamics. Nature 396:41–49.

Holland L, Dawson D, Horsburgh G, Krupa A, Stevens J (2013) Isolation and characterization of fourteen microsatellite loci from the endangered octocoral *Eunicella verrucosa* (Pallas 1766). Conservation Genet Resour 5:825–829.

Hu ZY, Doglioli AM, Petrenko AA, Marsaleix P, Dekeyser I (2009) Numerical simulations of eddies in the Gulf of Lion. Ocean Modelling 28:203–208.

Iacchei M, Ben-Horin T, Selkoe KA, Bird CE, Garcia-Rodrigues FJ, Toonen RJ (2013) Combined analyses of kinship and FST suggest potential drivers of chaotic genetic patchiness in high gene-flow populations. Mol Ecol 22:3476-3494.

Kinlan B, Gaines S (2003) Propagule dispersal in marine and terrestrial environments: a community perspective. Ecology 84:2007–2020.

Liggins L, Treml E, Riginos C (2013) Taking the plunge: an introduction to undertaking seascape genetic studies and using biophysical models. Geography Compass 7:173–196.

Linares C, Coma R, Garrabou J, Diaz D, Zabala M (2008) Size distribution, density and disturbance in two Mediterranean gorgonians: *Paramuricea clavata* and *Eunicella singularis*. Journal of Applied Ecology 45:688–699.

Manderson J (2016) Seascapes are not landscapes: an analysis performed using Bernhard Riemann's rules. ICES J. Mar. Sci. 73:1831–1838.

Manel S, Gaggiotti O, Waples R (2005) Assignment methods: matching biological questions with appropriate techniques. Trends in Ecology & Evolution 20:136–142.

Mantel N (1967) The Detection of Disease Clustering and a Generalized Regression Approach.

Cancer research 27(2) :209 -220

Millot C (1990) The Gulf of Lions' hydrodynamics. Continental shelf research 10:885–894.

Mitchell N, Dardeau M, Schaeffer W, Benke A (1992) Secondary production of gorgonian corals in the northern Gulf of Mexico. Marine Ecology Progress Series 87:275–281.

Mokhtar-Jamaï K, Pascual M, Ledoux JB, Coma R, Féral JP, Garrabou J, Aurelle D (2011) From global to local genetic structuring in the red gorgonian *Paramuricea clavata*: the interplay between oceanographic conditions and limited larval dispersal. Molecular Ecology 20:3291–3305.

Molecular Ecology Resources Primer Development Consortium (2010) Permanent genetic resources added to molecular ecology resources database 1 August 2009 - 30 September 2009. Molecular Ecology Resources 10:232–236.

Nanninga G, Saenz-Agudelo P, Manica A, Berumen ML (2014) Environmental gradients predict the genetic population structure of a coral reef fish in the Red Sea. Molecular Ecology 23:591–602.

Padrón M, Guizien K (2015) Modelling the effect of demographic traits and connectivity on the genetic structuration of marine metapopulations of sedentary benthic invertebrates. ICES

Journal of Marine Science. doi: 10.1093/icesjms/fsv158.

Paris C, Cherubin L, Cowen R (2007) Surfing, spinning, or diving from reef to reef: effects on population connectivity. Marine Ecology Progress Series 347:285–300.

Pineda J, Hare J, Sponaugle S (2007) Larval transport and dispersal in the coastal ocean and consequences for population connectivity. Oceanologica Acta 20:22–39.

Pritchard J, Stephens M, Donnelly P (2000) Inference of population structure using multilocus genotype data. Genetics 155:945–959.

Riginos C, Douglas K, Jin Y, Shanahan D, Treml E (2011) Effects of geography and life history traits on genetic differentiation in benthic marine fishes. Ecography 34:566–575.

Roberts C (1997) Connectivity and management of Caribbean coral reefs. Science 278:1454–1457.

Rossi V, Ser-Giacomi E, López C, Hernandez-García E (2014) Hydrodynamic provinces and oceanic connectivity from a transport network help designing marine reserves. Geophysical Research Letter 41:2883–2891.

Roughgarden J, Iwasa Y, Baxter C (1985) Demographic theory for an open marine population with space-limited recruitment. Ecology 66:54–67.

Ryman N, Palm S (2006) POWSIM: a computer program for assessing statistical power when testing for genetic differentiation. Molecular Ecology 6:600–602.

Selkoe K, Watson J, White C, Horin T, Iacchei M, Mitarai S, Siegel D, Gaines S, Toonen R (2010) Taking the chaos out of genetic patchiness: seascape genetics reveals ecological and oceanographic drivers of genetic patterns in three temperate reef species. Molecular Ecology

19:3708–3726.

Selkoe K, D'Aloia C, Crandall E, Iacchei M, Liggins L, Puritz J, Heyden von der S, Toonen R (2016) A decade of seascape genetics: contributions to basic and applied marine connectivity. Marine Ecology Progress Series 554:1–19.

Sexton J, Hangartner S, Hoffmann A (2013) Genetic isolation by environment or distance: which pattern of gene flow is most common? Evolution 68:1–15.

Shanks A, Grantham B, Carr M (2003) Propagule dispersal distance and the size and spacing of marine reserves. Ecological Applications 13:159–169.

Théodor J (1967) Contribution à l'étude des gorgones. VII. Ecologie et comportement de la planula. Vie Mileu 18:291–301.

Thomas L, Kennington W, Stat M, Wilkinson S, Kool J, Kendrick G (2015) Isolation by resistance across a complex coral reef seascape. Proceedings of the Royal Society B: Biological Sciences 282:20151217.

Treml E, Roberts J, Chao Y, Halpin P, Possingham H, Riginos C (2012) Reproductive output and duration of the pelagic larval stage determine seascape-wide connectivity of marine populations. Integrative and Comparative Biology 52:525–537.

Ulses C, Estournel C, Durrieu de Madron X, Palanques A (2008) Suspended sediment transport in the Gulf of Lions (NW Mediterranean): Impact of extreme storms and floods. Continental shelf research 28:2048–2070.

van Strien MJ, Holderegger R, Van Heck HJ (2015) Isolation-by-distance in landscapes: considerations for landscape genetics. 114:27–37.

552 Weersing K, Toonen R (2009) Population genetics, larval dispersal, and connectivity in marine
553 systems. Marine Ecology Progress Series 393:1–12.

554 Weinberg S (1978) Mediterranean octocorallian communities and the abiotic environment. Ma-
555 rine Biology 49:41–57.

556 Weinberg S, Weinberg F (1979) The life cycle of a gorgonian: *Eunicella singularis*. Bijdragen tot
557 de Dierkunde 48:1–14.

558 White C, Selkoe K, Watson J, Siegel D, Zacherl D, Toonen R (2010) Ocean currents help explain
559 population genetic structure. Proceedings of the Royal Society B: Biological Sciences
560 277:1685–1694.

561 Wilson G, Rannala B (2003) Bayesian inference of recent migration rates using multilocus geno-
562 types. Genetics 163:1177–1191.

563 Wright S (1931) Evolution in Mendelian populations. Genetics 16:97–159.

564 **Figure 1.-** Locations of sampling stations and habitat patches of *Eunicella singularis* in the Gulf
565 of Lion, NW Mediterranean. A) Black rectangles highlight the sampled habitat patches. Red areas
566 show the distribution of the rocky habitat in the region. B) Sampling stations of *E. singularis* and
567 rocky habitat extent in the Côte Bleue. C) Sampling stations of *E. singularis* and rocky habitat
568 extent in the Côte Vermeille. D) Sampling stations of *E. singularis* and rocky habitat extent in
569 Cap d'Agde and Plateau des Aresquiers. Red squares correspond to the areas of larval release
570 considered in the hydrological model. Sampling stations are represented by gray dots.
571 Information for each station is provided in Table 1.
572
573 **Figure 2.-** Plot of the Principal Coordinate Analysis (PCoA) from the genetic distance matrix
574 assessed with pairwise Nei's genetic distance estimates of *E. singularis* in the Gulf of Lion. The
575 first two axes explain 61.51% of the variation.
576
577 **Figure 3.-** Population structure of *E. singularis* in the Gulf of Lion, as revealed by Structure
578 software. Each individual is represented by a vertical color line, with each color representing the
579 proportion of membership to each cluster. Black lines represent the division among the identified
580 clusters (K = 3). Values between parentheses correspond to the overall proportion of membership
581 of the individuals in each cluster.
582
583 **Figure 4.-** Patterns of contemporary migration among habitat patches of *Eunicella singularis* in
584 the Gulf of Lion. The matrix shows the number of migrants coming from any potential source and
585 reaching any destination habitat patch. CV = Côte Vermeille, CA = Cap d'Agde, PA = Plateau
586 des Aresquiers, and CB = Côte Bleue. The number of migrants between any two habitat patches
587 is represented by the grayscale intensity.
588

Figure 5.- A) Relationship between the number of emigrants (sum of number of migrants by row) from a source habitat patch and the population density in that source habitat patch. B) Relationship between the number of immigrants (sum of number of migrants by column) to a destination habitat patch and the population density in that destination habitat patch. X error bars correspond to the standard deviation around the mean population density values. Y error bars correspond to the confidence intervals around the number of migrants estimated by BayesAss.

Figure 6.- Patterns of recent larval transport and contemporary gene flow among habitat patches of *E. singularis* in the Gulf of Lion. A) Recent larval transport for a PLD of 3.5 days; B) recent larval transport for a PLD of 7 days; C) recent larval transport for a PLD of 10.5 days; D) recent larval transport for a PLD of 14 days; E) recent larval transport for a PLD of 21 days; F) contemporary gene flow. The Grayscale indicates the probability values.

Figure 7.- Determination coefficient between contemporary gene flow and recent larval transport (including retention rates) for a PLD ranging from 3.5 to 42 days. Filled circles depict the PLDs for which the Mantel test showed significant correlations between contemporary gene flow and recent larval transport matrices, excluding retention rates.

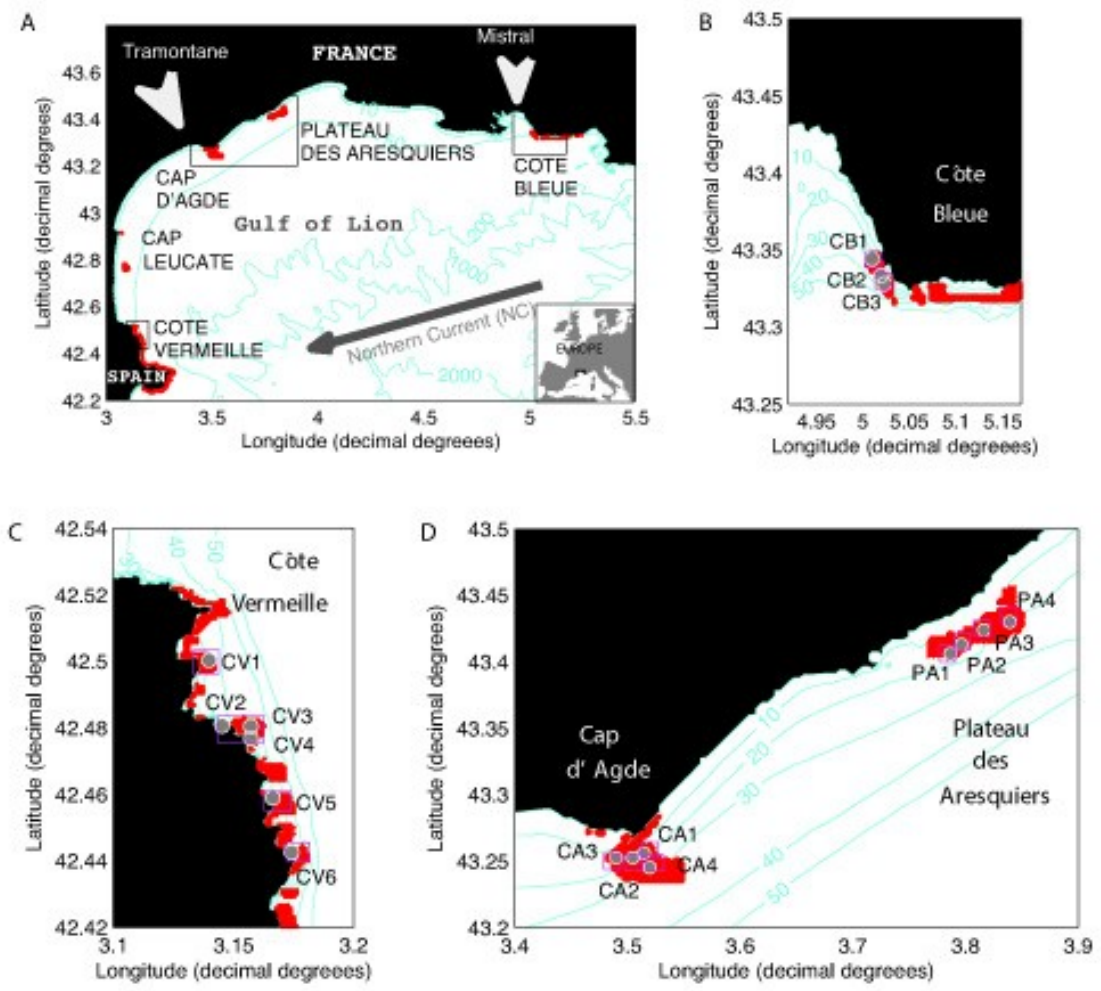

Figure 1.-Locations of sampling stations and habitat patches of *Eunicella singularis* in the Gulf of Lion, NW Mediterranean. A) Black rectangles highlight the sampled habitat patches. Red areas show the distribution of the rocky habitat in the region. B) Sampling stations of *E. singularis* and rocky habitat extent in the Côte Bleue. C) Sampling stations of *E. singularis* and rocky habitat extent in the Côte Vermeille. D) Sampling stations of *E. singularis* and rocky habitat extent in Cap d'Agde and Plateau des Aresquiers. Red squares correspond to the areas of larval release considered in the hydrological model. Sampling stations are represented by gray dots. Information for each station is provided in Table 1.

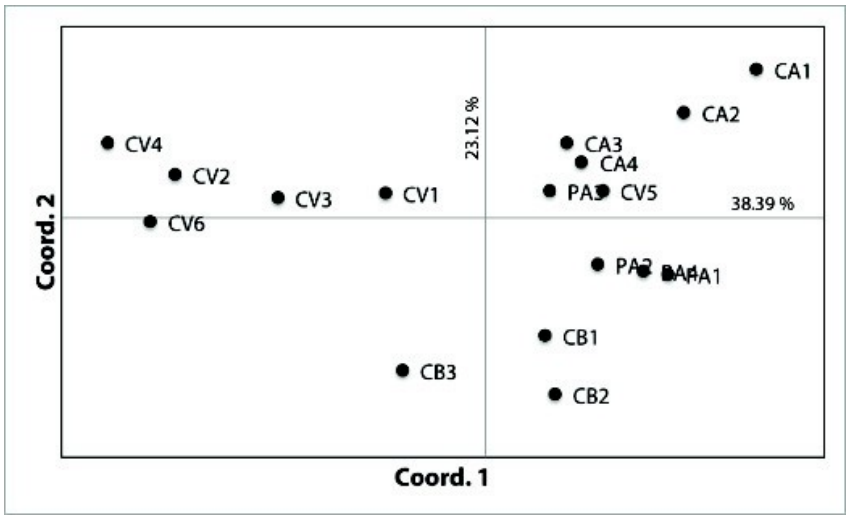

Figure 2.- Plot of the Principal Coordinate Analysis (PCoA) from the genetic distance matrix assessed with pairwise Nei's genetic distance estimates of *E. singularis* in the Gulf of Lion. The first two axes explain 61.51% of the variation.

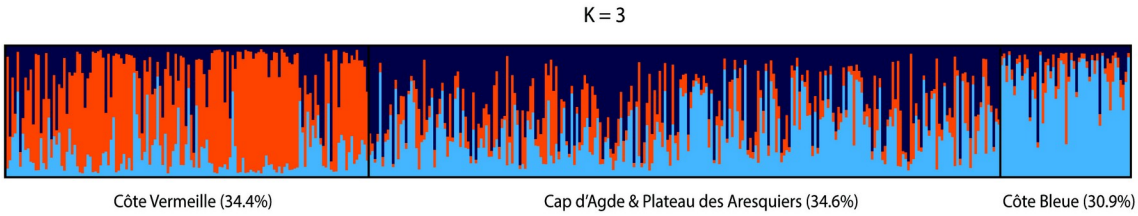

Figure 3.- Population structure of *E. singularis* in the Gulf of Lion, as revealed by Structure software. Each individual is represented by a vertical color line, with each color representing the proportion of membership to each cluster. Black lines represent the division among the identified clusters (K = 3). Values between parentheses correspond to the overall proportion of membership of the individuals in each cluster.

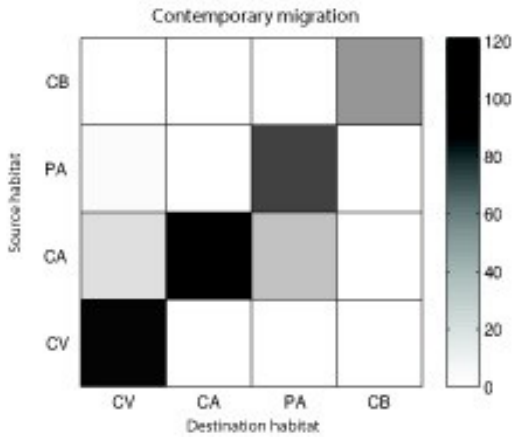

Figure 4.- Patterns of contemporary migration among habitat patches of *Eunicella singularis* in the Gulf of Lion. The matrix shows the number of migrants coming from any potential source and reaching any destination habitat patch. CV = Côte Vermeille, CA = Cap d'Agde, PA = Plateau des Aresquiers, and CB = Côte Bleue. The number of migrants between any two habitat patches is represented by the grayscale intensity.

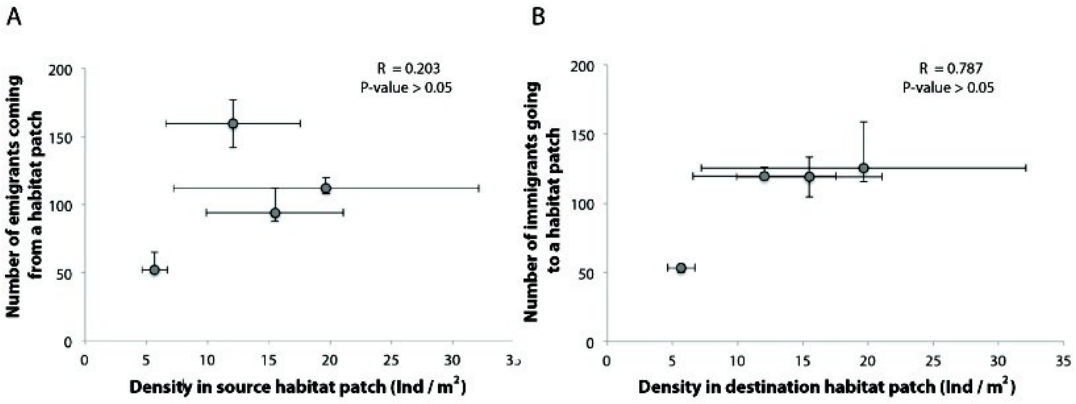

Figure 5.- A) Relationship between the number of emigrants (sum of number of migrants by row) from a source habitat patch and the population density in that source habitat patch. B) Relationship between the number of immigrants (sum of number of migrants by column) to a destination habitat patch and the population density in that destination habitat patch. X error bars correspond to the standard deviation around the mean population density values. Y error bars correspond to the confidence intervals around the number of migrants estimated by BayesAss.

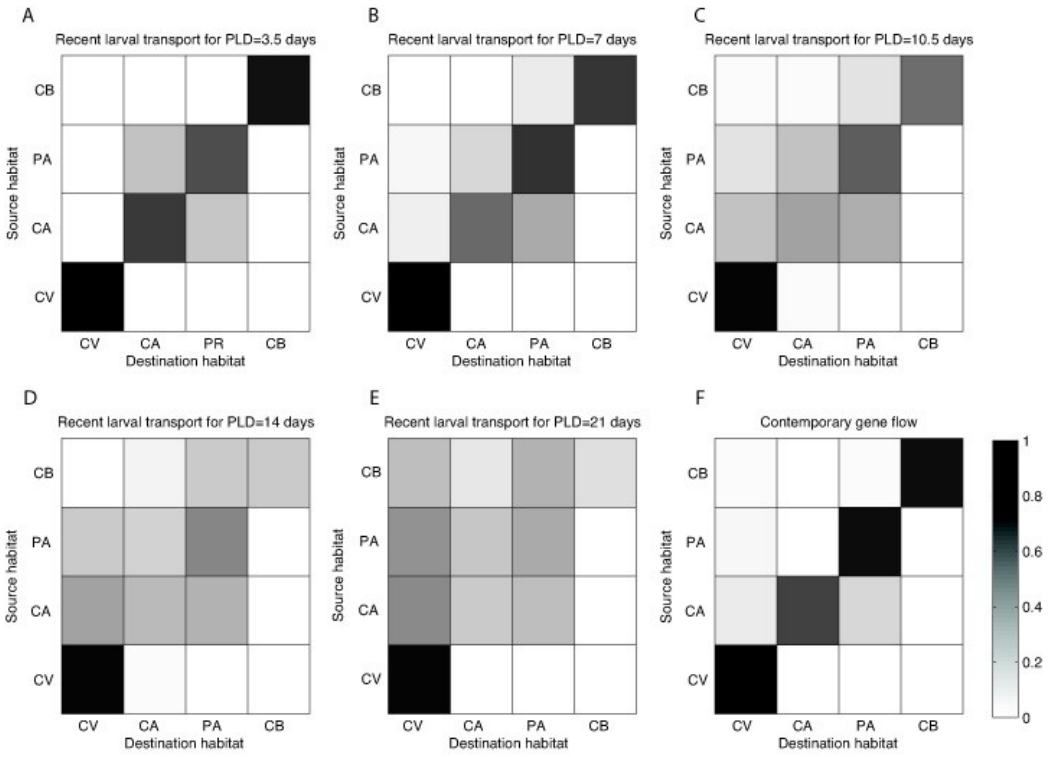

Figure 6.- Patterns of recent larval transport and contemporary gene flow among habitat patches of *E. singularis* in the Gulf of Lion. A) Recent larval transport for a PLD of 3.5 days; B) recent larval transport for a PLD of 7 days; C) recent larval transport for a PLD of 10.5 days; D) recent larval transport for a PLD of 14 days; E) recent larval transport for a PLD of 21 days; F) contemporary gene flow. The Grayscale indicates the probability values.

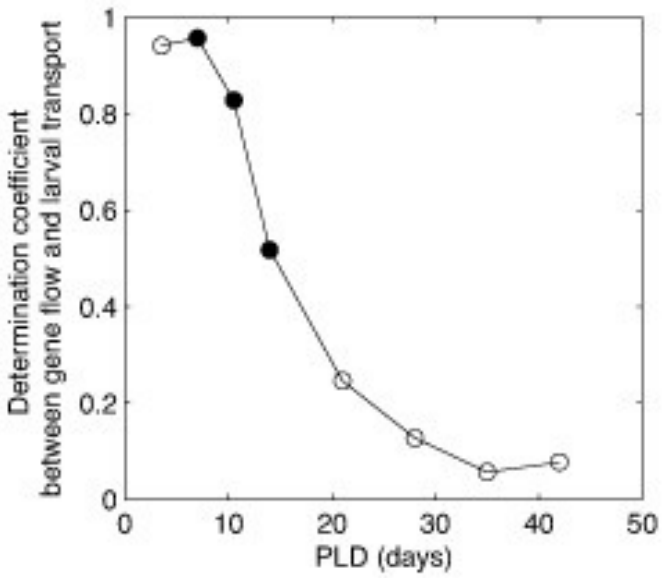

Figure 7.- Determination coefficient between contemporary gene flow and recent larval transport (including retention rates) for a PLD ranging from 3.5 to 42 days. Filled circles depict the PLDs for which the Mantel test showed significant correlations between contemporary gene flow and recent larval transport matrices, excluding retention rates.